

2

This is a preprint of a paper intended for publication in a journal or proceedings. Since changes may be made before publication, this preprint is made available with the understanding that it will not be cited or reproduced without the permission of the author.

UCRL - 77310

PREPRINT

Conf-750975--5



LAWRENCE LIVERMORE LABORATORY

University of California / Livermore, California

Measurement of X-Rays Emitted  
from Projectiles Moving in Solid Targets

R. J. Fortner

D. L. Matthews

L. C. Feldman

J. D. Garcia

H. Oona

September 1975

NOTICE

This report was prepared as an account of work sponsored by the United States Government. Neither the United States nor the United States Energy Research and Development Administration, nor any of their employees, nor any of their contractors, subcontractors, or their employees, make any warranty, express or implied, or assume any legal liability or responsibility for the accuracy, completeness or usefulness of any information, apparatus, product or process disclosed, or represents that its use would not infringe privately owned rights.

This paper was prepared for submission to  
4th International Conference  
Beam-Foil Spectroscopy and Heavy Ion Atomic Physics  
Gatlinburg, Tennessee September 15 - 19, 1975

DISTRIBUTION OF THIS DOCUMENT IS UNLIMITED

109

MEASUREMENT OF X-RAYS EMITTED FROM PROJECTILES MOVING IN  
SOLID TARGETS\*

R. J. Fortner and D. L. Matthews  
Lawrence Livermore Laboratory  
Livermore, California 94550

L. C. Feldman  
Bell Telephone Laboratories  
Murray Hill, New Jersey 07974

J. D. Garcia and H. Oona  
University of Arizona  
Tucson, Arizona 85721

ABSTRACT

In this paper the results of three separate experiments all dealing with the production of x-rays in projectiles moving in solids will be discussed. The first experiment<sup>1</sup> deals with the measurement of line widths of x-rays emitted from projectiles moving in solid targets. The effects of collisionally broadening of x-rays is found to dominate the line widths giving greater than an order of magnitude increase in the measured line widths. The second experiment<sup>2</sup> studies "solid target effects" in producing non-binomial distributions of characteristic K x-ray spectra in heavy ion-atom collisions. The third experiment<sup>3</sup> studies aluminum K x-ray production in  $Ar^{14+}$  Al collisions in very thin aluminum foils as a function of foil thickness. Parameterization of the observed non-linear dependence enables us to measure the lifetime of the argon 2p vacancy and total ionization cross sections for the argon L-shell in  $Ar + Al$  collisions.

\*Work performed under the auspices of the United States Energy Research and Development Administration, under contract No. W-7405-Eng-48.

## 1. COLLISIONAL BROADENING OF X-RAYS

In Fig. 1b and 1c the neon K x-ray spectra for 3 types of collisions, 1.3 keV electrons incident on a neon gas target, and 90 keV neon ions incident on a neon gas target and a solid copper target. The gas target (Fig. 1c) spectra exhibit clean well resolved peaks and the origins of these peaks have been discussed extensively in the literature. Basically each line corresponds to an initial state involving one K-shell vacancy and fixed ionization in the L-shell. The peaks are designated as such in the figure where  $KL^n$  corresponds to the x-ray transition from an initial state having one K-shell vacancy and n L-shell vacancies. However, these well resolved discrete peaks are not observed for the neon K x-ray spectra emanating from ions moving in solid copper targets (Fig. 1b). The peak of this spectra occurs in the region of the normal  $KL^0$  peak; however, the peak extends in energy over a very broad energy range with essentially no structure detectable in the spectra. This spectra is skewed toward the high energy side, probably indicating the existence of states of excitation higher than  $KL^0$ . On the low energy side of  $KL^0$  the spectra extends to lower energies indicating that the individual lines are considerably broadened.

In Fig. 2 the boron K x-ray spectra for 2 types of boron-carbon collisions are presented. The first spectra is for a methane gas target. Basically the x-ray lines are from boron coming primarily from electron transitions in one, two, and three electron atoms. The second spectra is for a solid diamond target. The most obvious difference is the large carbon K line which dominates the solid target spectra but is not observed in a gas target. This peak occurs in the solid targets because of recoiling carbon atoms and subsequent C-C collisions. A more important difference with respect to this paper is the x-ray transitions emanating from the boron projectile. For the solid target only two broad continuous x-ray bands in the region where boron K x-ray transitions are expected are observed. The identification of the two bands is straightforward. The low energy band, centered near 190 eV, is consistent with calculations of the  $2p \rightarrow 1s$  x-ray transitions in atoms having initial states involving one K-shell vacancy and one, two or three electrons in the L-shell. The second higher energy band, centered near 245 eV on the low energy tail of the carbon K x-ray is consistent with  $2p \rightarrow 1s$  transitions in atoms having two K-shell vacancies in the initial state and one, two or three L-shell electrons. The significant point to be extracted from both Fig. 1b and Fig. 2 concerns the widths of the x-ray lines obtained from the projectiles moving in solid targets. In both figures the data obtained from gas target spectra exhibit clearly resolved peaks. However, when the x-ray spectra are measured using the same instrumental resolution for ions moving in a solid target all the sharply resolved x-ray structure disappears and only broad x-ray bands are resolved. This

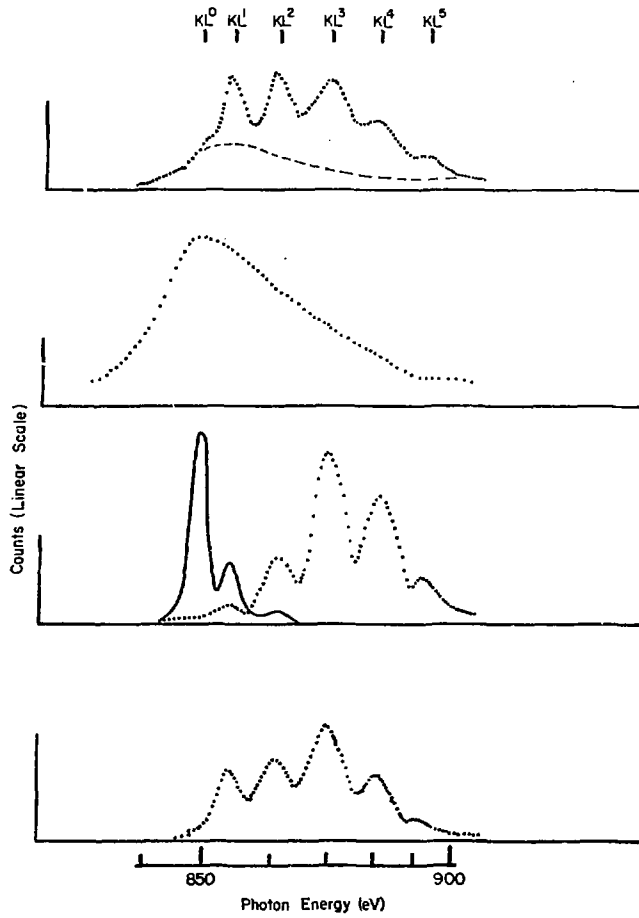


Figure 1

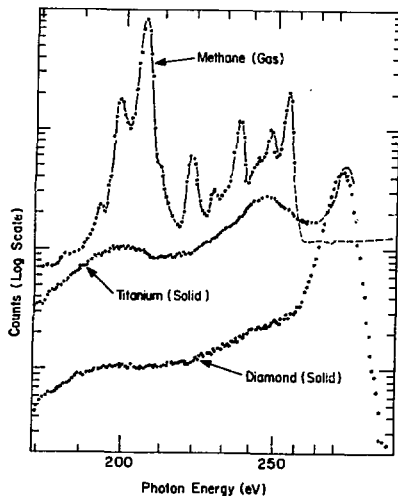


Figure 2

broadening of the x-rays in the solid is the x-ray analog to the collisional broadening of spectral lines observed in dense plasmas. It is the result of a disruption in the radiation field of the inner shell vacancy induced by multiple collisions which take place prior to the filling of the x-ray transition.

An estimate of the size of the collisional x-ray broadening can be obtained by unfolding the x-ray spectra in Fig. 1b and 2. In this unfolding of the data we used Gaussian line shapes and centroid energies as observed in gas target measurements. This unfolding of the  $\text{Ne}^I \rightarrow \text{Cu}$  spectra indicated a width of  $12 \pm 3$  eV for the peaks  $\text{KL}^0$  to  $\text{KL}^4$  respectively. The boron K x-ray spectra were unfolded using the double K-shell vacancy peak from Fig. 2b. The spectra indicated a width of  $12 \pm 5$  eV and equal intensities of the  $\text{K}^2\text{L}^0$  and  $\text{K}^2\text{L}^1$  x-ray peaks.

## 2. NON BINOMIAL DISTRIBUTIONS OF HEAVY-ION INDUCED NEON K X-RAY SPECTRA

In Fig. 1a the neon K x-ray spectra produced in collisions of neon ions incident on a graphite (carbon) thick target. The spectra was observed only after long bombardment of neon ions and thus is attributed to Ne - Ne collisions taking place in the carbon solid. This spectra is expected to have two components; one from a moving neon projectile, and the second from implanted neon atoms at rest in the graphite. The projectile spectra is broadened as in Fig. 1b and the target spectra shows peaks. The dashed line in Fig. 1a indicates our estimate of the projectile contribution obtained by normalizing the spectra shown in Fig. 1b to the low energy part of the spectra in Fig. 1a. The difference spectra which would be associated with the implanted neon target is shown in Fig. 1d. Notice the difference in the two neon-neon spectra for a gas target (1c) and a solid target (1d). The x-ray line intensities from the gas target spectra are binomial in character and for the solid target spectra they are not. We can attribute this difference to the capture of target electrons into excited states when the neon is in the carbon solid. These electrons can auto-ionize filling L-shell vacancies prior to the K x-ray decay which then results in fewer number of L-shell vacancies as observed in the x-ray spectra and a non-binomial distribution.

## 3. LIFETIME STUDIES OF Ar-2p VACANCIES TRAVELING THROUGH SOLIDS

We report studies on the production of aluminum K x-rays in Ar-Al collisions using varying thicknesses of thin aluminum foils. It has been suggested that the mechanism for aluminum K vacancy production requires two collisions; the first collision produces an argon 2p vacancy in the argon projectile and the second collision transfers this 2p vacancy to the 1s level of the aluminum. The reasons for interest in these studies is that in very thin foils, i.e., thickness less than  $v\tau$  where  $v$  is the velocity of the ion and  $\tau$  is the lifetime of the argon L vacancy, the aluminum K yield is not a linear function of thickness and the shape of the curve will depend on the lifetime of the argon 2p vacancy. Thus, parameterization of this data enables us to infer an average lifetime for the argon 2p vacancy traveling through a solid.

The experiments used thin foils of carbon of thickness  $\sim 10 \mu\text{g}/\text{cm}^2$  with thin evaporated layers of aluminum ranging from 60 Å to 333 Å. In the first experiment the yield of aluminum K x-rays was measured for the argon beam incident, first on the carbon side and then on the aluminum side of the foil. Those yields are displayed in Fig. 3 as a function of energy. The aluminum yield for argon first traveling through carbon is considerably higher since there

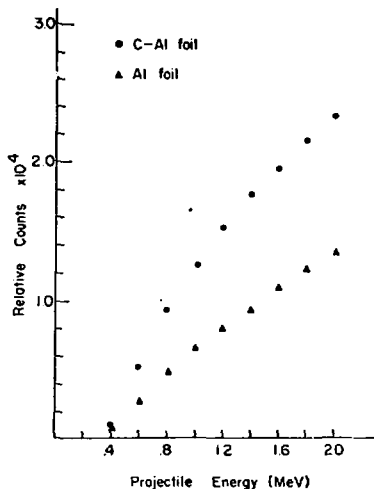


Figure 3

is a large steady state distribution of argon L vacancies established in this beam prior to penetration into aluminum. This observation confirms the basic explanation of Al-Ls vacancy production mechanism discussed above.

In a second set of measurements the yield of aluminum K x-rays was measured as a function of aluminum thickness ( $T$ ) by using different foils and various angles to the beam. In this case the fraction of beam with L vacancies,  $f_1(t)$  at depth  $t$ , now due to Ar-Al collisions may be written as

$$f_1(t) = \frac{N\sigma v_T}{1+N\sigma v_T} \left(1 - e^{-\left(N\sigma + \frac{1}{v_T}\right)t}\right)$$

where  $N$  is the atom density of Al,  $\sigma$  the cross section for argon L vacancy production. Then the total yield of Al,  $Y_{Al}$ , is proportional to

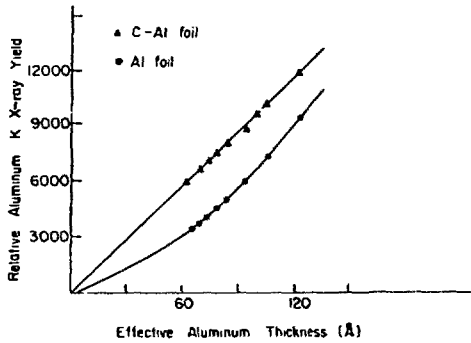


Figure 4

$$Y_{Al} = \int_0^T f_1(t)dt = \left[ T + \frac{e^{-(N\sigma + \frac{1}{V\tau})T} - 1}{N\sigma + \frac{1}{V\tau}} \right]$$

In Fig. 4 the yield of aluminum K x-rays as a function of foil thickness is shown. The data for the aluminum foils clearly shows the non-linear dependence of the aluminum K x-ray yield on foil thickness. Parameterization of these data enabled us to determine independently both  $\sigma$  and  $\tau$ . A summary of the values of  $\tau$  and  $\sigma$  obtained for a variety of projectile energies is shown in Table 1.



TABLE I

<u>Energy</u> <u>(Mev)</u>	$\sigma$ <u>(<math>\times 10^{-17}</math> cm<sup>2</sup>)</u>	$\tau$ <u>(<math>\times 10^{-15}</math> sec)</u>
.3	.35	1.50 ( $\pm .30$ )
.4	.59	2.15 ( $\pm .44$ )
.5	.90	4.8 ( $\pm .5$ )
1.0	1.58	11.0 ( $\pm 2.5$ )
1.5	3.10	20. ( $\pm 20$ )
2.0	4.10	-----

## REFERENCES

1. R. J. Fortner, D. L. Matthews, J. D. Garcia and H. Oona (to be published).
2. R. J. Fortner and D. L. Matthews (to be published).
3. L. C. Feldman, R. A. Levesque, P. J. Silverman and R. J. Fortner (to be published).